ORGANIC LETTERS

2000
Vol. 2, No. 21
3313−3316

Conformational Study of the Intramolecular Diels–Alder Reaction of a Pentadienyl Acrylate. Theoretical Evaluation of Kinetic and Thermodynamic Control

James D. White,*,† F. W. J. Demnitz,† Hirohisa Oda,† Carla Hassler,† and James P. Snyder*,‡

Departments of Chemistry, Oregon State University, Corvallis, Oregon 97331-4003, and Emory University, Atlanta, Georgia 30322

james.white@orst.edu

Received July 26, 2000

ABSTRACT

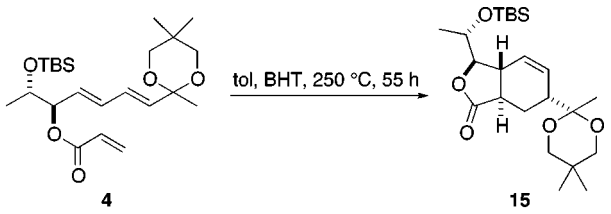

Acrylate 4, prepared from diacetylrhamnal, underwent intramolecular Diels–Alder cycloaddition to give the thermodynamically disfavored trans-fused γ-lactone 15 as the major product, along with two stereoisomeric cycloadducts. A computational analysis of each of the four transition states arising from 4 and the corresponding cycloadducts permits an understanding of the contrasting requirements for kinetic versus thermodynamic control of the reaction.

A key step in our approach to the synthesis of pillaromycinone (**1**),[1] the aglycone of the anthracycline antibiotic pillaromycin A (**2**),[2] is an intramolecular Diels−Alder reaction which establishes the A ring and sets in place the components necessary to fabricate ring B.[3,4] Since all of the stereochemical features of **1** reside in either ring A or at its fusion with ring B, stereocontrol in the intramolecular Diels−Alder process which elaborates the AB substructure becomes a critical factor in our progress toward an asymmetric synthesis of **1**.

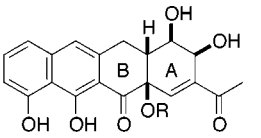

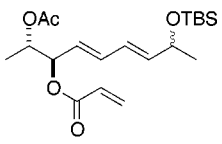

It is well-known that stereocenter(s) external to the core unit undergoing intramolecular Diels−Alder cycloaddition

† Oregon State University.
‡ Emory University.

(1) (a) Asai, M.; Mizuta, E.; Mizuno, K.; Miyake, A.; Tatsuoka, S. *Chem. Pharm. Bull. Jpn.* **1970**, *18*, 1720. (b) Pezzanite, J. O.; Clardy, J.; Lou, P.-Y.; Wood, G.; Walker, D. L.; Fraser-Reid, B. O. *J. Am. Chem. Soc.* **1975**, *97*, 6250.

(2) (a) Asai, M. *Chem. Pharm. Bull. Jpn.* **1970**, *18*, 1699. (b) Kamiya, K.; Asai, M.; Nishikawa, M.; Mizuno, K.; Tomiie, Y.; Nitta, I. *Chem. Pharm Bull. Jpn.* **1970**, *18*, 1724.

(3) White, J. D.; Nolen, E. G.; Miller, C. H. *J. Org. Chem.* **1986**, *51*, 1150.

(4) For a different approach to **1**, see: (a) Trost, B. M.; Caldwell, C. G.; Murayama, E.; Heissler, D. *J. Org. Chem.* **1983**, *48*, 3252. (b) Majuindar, G.; Pal, R.; Murty, K. V. S. M.; Mal, D. *J. Chem. Soc., Perkin Trans. 1* **1994**, 309.

10.1021/ol000200f CCC: $19.00
Published on Web 09/29/2000

can exert a powerful influence on the course of the reaction.[5] In the case of **3**, we observed that three of the four possible stereoisomeric cycloadduct pairs were produced,[3] but accurate quantitative evaluation of the reaction mixture was complicated by the fact that epimers of **3** as well as stereoisomers of the products were inseparable. Furthermore, no clear-cut rationale could be derived from the reaction of **3** which allowed predictive assessment of the stereochemical outcome of related intramolecular Diels−Alder cycloadditions.[6] Nevertheless, it was evident that stereochemical information was being transmitted from existing centers in the substrate **3** to new centers in the cycloadducts. This process, which we have termed "stereochemical transcription",[3] is a valuable means for augmenting stereochemical content in synthesis. In principle, it should operate with good fidelity in reactions such as the intramolecular Diels−Alder reaction which proceed via a compact transition state.

Two recent studies of conformational effects on the intramolecular Diels−Alder reaction of hexadienyl acrylates[7,8] prompt us to report our results with pentadienyl acrylate **4**. With this substrate, the ambiguity present in the cycloaddition of the stereoisomeric mixture **3** is removed, thus permitting a more accurate assessment of products from the cycloaddition. Acrylate **4** was synthesized from diacetylrhamnal (**5**), obtained from L-rhamnose,[9] as shown in Scheme 1. After conversion of **5** to dienone **6**,[3] the secondary alcohol

Scheme 1

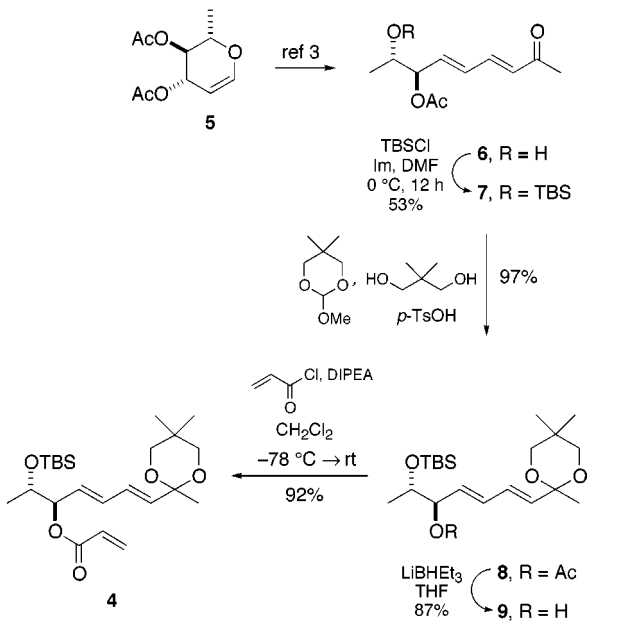

was protected as its silyl ether **7**. Ketalization in the presence of 2,2-dimethylpropane-1,3-diol gave **8**, from which the acetyl group was removed to yield alcohol **9**. Esterification with acryloyl chloride then afforded **4**.

To simplify computational analysis of the intramolecular Diels−Alder reaction of **4**, the *tert*-butyldimethylsilyl residue was replaced with $SiMe_3$ as in **10** (Table 1). Then, each of the exo and endo transition states implied by the rotamers

Table 1. Relative Energies of Transition States and Diels−Alder Products Derived from Reacting Conformations of **10** Using Becke3LYP/6-31G*//MM3* and Becke 3LYP/3-21G//MM3*

Conformation	Relative Energy of TS (kcal/mol)	Product	Relative Energy of Product (kcal/mol)
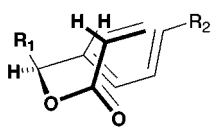 β-*endo*	2.4[a] (1.4)[b]	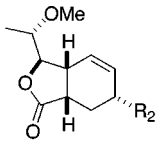 **11**	(0.0)[a] (0.0)[b]
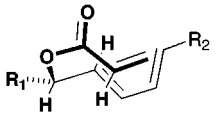 β-*exo*	0.0[a] (0.0)[b]	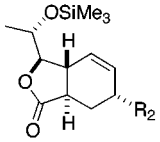 **12**	6.1[a] (7.9)[b]
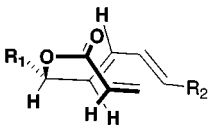 α-*endo*	2.4[a] (2.3)[b]	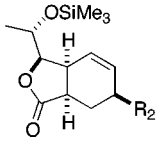 **13**	4.9[a] (5.0)[b]
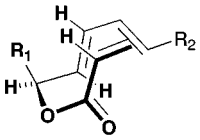 α-*exo*	8.2[a] (7.5)[b]	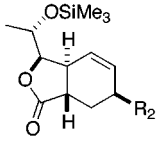 **14**	10.7[a] (11.1)[b]

10, R_1 = 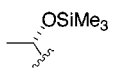 R_2 = 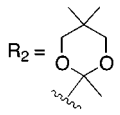

[a] Becke3LYP/6-31G*//MM3*. [b] Becke 3LYP/3-21G//MM3*.

of **10** depicted in Table 1 was subjected to a Monte Carlo MCMM conformational search in MacroModel6.5[10,11] employing the MM2* parameters of Raimondi and co-workers[12] and the GBSA/$CHCl_3$ solvation model.[13] Single point energies of the respective global minima were obtained by density functional theory (DFT) at the Becke3LYP/3-21G and Becke3LYP/6-31G* levels with Gaussian 98.[14] The β-exo conformation is predicted to correspond to the lowest energy cycloaddition pathway, whereas the α-exo corresponds to the highest. β-Endo and α-endo pathways are computed to have similar energies and to fall between the two extremes (Table 1). Relative Boltzmann populations of the products estimated by relative Becke3LYP/6-31G* TS energies for β-exo, β-endo, α-endo, and α-exo conformations at 250 °C are 2.3:0.2:0.2:0.06, respectively.

As shown for the β-exo TS in Figure 1, the four transition states sustain a relatively long bond at the incipient lactone ring and a shorter separation at the ketal substitution site

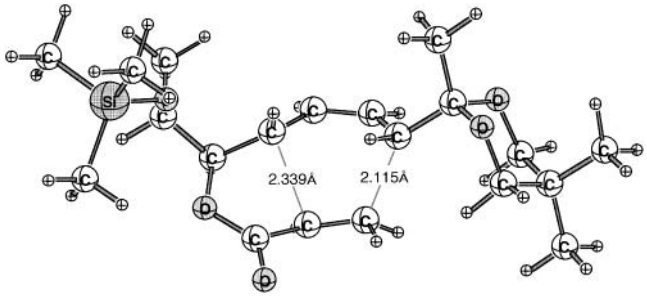

Figure 1. The MM2* optimized β-exo transition state for **10**.

(i.e., 2.339−2.349 and 2.113−2.115 Å). Isomer energy differences appear to be largely due to steric effects. All of the transition structures are crowded, containing a number of short atomic contacts (2.2−2.6 Å) between the exocyclic substituents and the forming bicycle.[15] However, the β-exo structure has fewer and longer contacts that apparently endow it with the greatest stability.

The calculated energies for the MM2* conformational global minima for the four cycloadducts **11**−**14** arising from **10** are also given in Table 1. The data in this table leads to the clear prediction that cis-fused lactone **11**, the product of β-endo cycloaddition of **10**, should be the most stable of the four cycloadducts. While structure **11** experiences one short H−H contact from the bridgehead, both bridgehead protons of **12** engage in similarly short H−O interactions. If the reaction is under kinetic control, the less stable β-exo trans-fused isomer **12** should be the favored product. It is also apparent from these data that trans-fused α-exo lactone **14** should be highly disfavored on steric grounds.

An experimental test of these predictions was carried out by heating **4** in toluene at 250 °C in the presence of BHT. This resulted in the formation of three cycloadducts in the ratio 2.3:1.4:1.0 which were identified as **15**, **16**, and **17**, originating from β-exo, β-endo, and α-endo modes of cycloaddition, respectively (Scheme 2).

Scheme 2

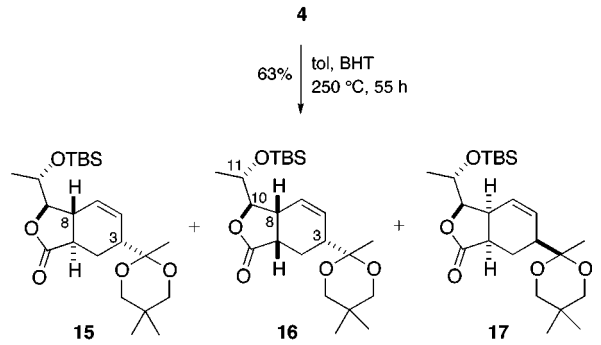

All three adducts were stable under the reaction conditions. No trace of a fourth Diels−Alder product from α-exo

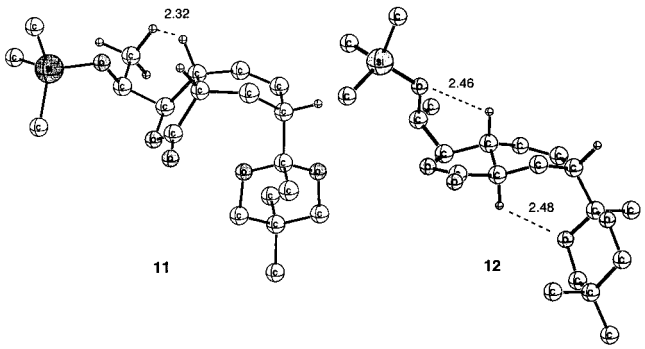

Figure 2. Calculated minimum energy conformations (MM2*) of β-endo and β-exo products **11** and **12**.

cycloaddition was found in the reaction mixture, in agreement with the prediction from computational analysis. The crystalline cis-fused lactone **16** readily yielded to an X-ray crystallographic determination of its structure (Figure 3)

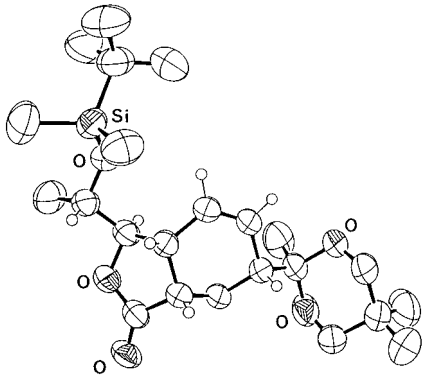

Figure 3. X-ray crystal structure of **16**. Elllipsoids are drawn at the 30% probability level.

which is characterized by an anti,anti arrangement of hydrogens at C8, C10, and C11. Trans-fused lactone **15** was isomerized quantitatively to the cis-fused structure **16** under basic conditions (NaH, $(i\text{-Pr})_2$NEt), supporting the configurational assignments made to C3 and C8 of **15** as well as

(5) Craig, D. *Chem. Soc. Rev.* **1987**, *16*, 187.
(6) For studies of the intramolecular Diels−Alder reaction of pentadienyl citraconates, see: (a) White, J. D.; Sheldon, B. G.; Solheim, B. A.; Clardy, J. *Tetrahedron Lett.* **1978**, 5189. (b) White, J. D.; Sheldon, B. G. *J. Org. Chem.* **1981**, *46*, 2273. (c) White, J. D. *Proceedings of the Sino-American Symposium on the Chemistry of Natural Products*; Yu, W., Ed.; Science Press: Beijing, China, 1981; pp 146−149.
(7) Kim, P.; Nantz, M. H.; Kurth, M. J.; Olmstead, M. M. *Org. Lett.* **2000**, *2*, 1831.
(8) Jung, M. E.; Huang, A.; Johnson, T. W. *Org. Lett.* **2000**, *2*, 1835.
(9) Roth, W.; Pigman, W. *Methods Carbohydr. Chem.* **1963**, *2*, 405.
(10) (a) Mohamadi, F.; Richards, N. G. J.; Guida, W. C.; Liscamp, R.; Lipton, M.; Caufield, C.; Chang, G.; Hendrickson, T.; Still, W. C. *J. Comput. Chem.* **1990**, *11*, 440. (b) Cf. http://www.schrodinger.com/macromodel2.html.
(11) Chang, G.; Guida, W. C.; Still, W. C. *J. Am. Chem. Soc.* **1989**, *11*, 4379.

the calculated thermodynamic stabilities of **11** and **12** shown in Table 1. Confirmation of the relative stereochemistry of **15** was obtained after osmylation, which occurred exclusively from the β face of the alkene, followed by ketalization of the resultant diol **18** (Scheme 3). X-ray analysis of crystalline

Scheme 3

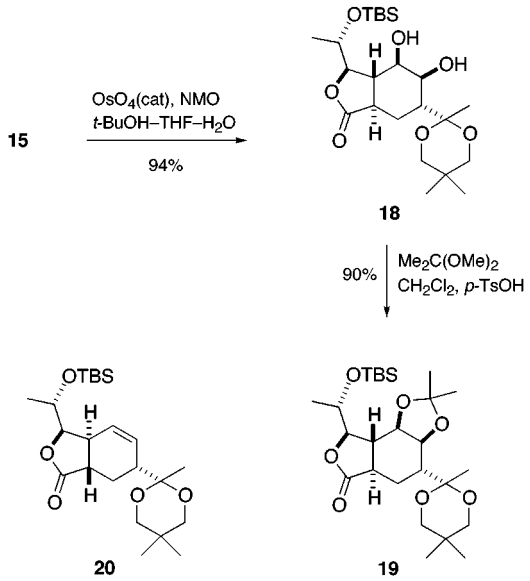

ketal **19** revealed the structure shown in Figure 4. Both **18** and **19** displayed a large (14 Hz) coupling constant between the ring fusion protons, whereas cis-fused isomers **16** and **17** showed a smaller coupling (9 Hz) between these hydrogens. Although the trans-fused isomer **20** corresponding to **14** was not observed among the cycloadducts from **4**, it was detected by ^{1}H and ^{13}C NMR as a minor component in a mixture with **17** after equilibration of the latter with base.

In summary, the ratio of products **15**−**17** obtained from **4** is closely matched by the combined force field and DFT calculations. The latter predict both the major kinetic and thermodynamic products from **4** and provide a rationale for the differences. Importantly, lactone **16**, which can also be obtained by isomerization of **15**, has the desired absolute configuration for advancement toward **1**.

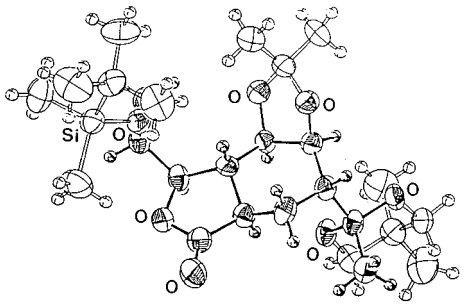

Figure 4. X-ray crystal structure of **19**. Elllipsoids are drawn at the 30% probability level.

Acknowledgment. We are grateful to Professor Alex Yokochi, Oregon State University, for the X-ray crystal structures of **16** and **19**. Financial support was provided by the National Science Foundation (Grants 9711187-CHE and 0076103-CHE).

Supporting Information Available: X-ray crystallographic data for **16** and **19**; characterization data for **15**, **16**, **17**, **18**, and **19**. This material is available free of charge via the Internet at http://pubs.acs.org.

OL000200F

(12) Raimondi, L.; Brown, F. K.; Gonzalez, J.; Houk, K. N. *J. Am. Chem. Soc.* **1992**, *112*, 4796.

(13) Still, W. C.; Tempczyk, A.; Hawley, R. C.; Hendrickson, T. *J. Am. Chem. Soc.* **1990**, *112*, 6127.

(14) *Gaussian 98* (Revision A). Frisch, M. J.; et al.; Gaussian, Inc., Pittsburgh, PA, 1998.

(15) The best value for the van der Waals radius of C−H hydrogen is 1.2 Å (Bondi, A. *J. Phys. Chem.* **1964**, *68*, 441. Rowland, R. S.; Taylor, R. *J. Phys. Chem.* **1996**, *100*, 7384), implying that r(H···H) = 2.4 Å is at the contact boundary.